

The nuclear electric polarizability of ${}^6\text{He}$

R. Goerke,^{1,2,*} S. Bacca,^{2,†} and N. Barnea^{3,‡}

¹*Department of Physics, University of Toronto, 60 St. George St., Toronto, Ontario, M5S 1A7, Canada*

²*TRIUMF, 4004 Wesbrook Mall, Vancouver, BC, V6T 2A3, Canada*

³*Racah Institute of Physics, Hebrew University, 91904, Jerusalem, Israel*

(Dated: August 6, 2018)

We present an estimate of the nuclear electric polarizability of the ${}^6\text{He}$ halo nucleus based on six-body microscopic calculations. Wave functions are obtained from semi-realistic two-body interactions using the hyperspherical harmonics expansion method. The polarizability is calculated as a sum rule of the dipole response function using the Lanczos algorithm and also by integrating the photo-absorption cross section calculated via the Lorentz integral transform method. We obtain $\alpha_E = 1.00(14) \text{ fm}^3$, which is much smaller than the published value $\alpha_E^{\text{exp}} = 1.99(40) \text{ fm}^3$ [1] extracted from experimental data. This points towards a potential disagreement between microscopic theories and experimental observations.

PACS numbers: 21.10.Gv, 24.70.+s, 21.60.De, 27.20.+n

I. INTRODUCTION

The nuclear electric polarizability α_E is related to the response of a nucleus to an externally applied electric field. It is an interesting observable because it encapsulates information about the excitation spectrum of a nucleus. Recently, it has attracted a lot of attention both for light nuclei, see *e.g.* [1], and for heavy nuclei, see *e.g.* [2]. For light systems the nuclear polarizability is relevant in the extraction of nuclear quantities from atomic spectroscopic measurements. The atomic energy levels are affected by polarization of the nucleus due to the electric field of the surrounding electrons. Such nuclear structure correction, which is proportional to $Z^3\alpha_E/a_0$ [3] where a_0 is the Bohr radius, needs to be considered in the sophisticated quantum electrodynamics calculations of the atomic levels that allow the extraction of charge radii from isotope shifts measurements of unstable nuclei, see Refs. [4, 5] and [6] for ${}^6\text{He}$ and ${}^8\text{He}$, respectively. An even larger effect of the nuclear structure correction coming from the polarizability is expected in muonic atoms, as the muon mass is larger than the electron mass and the orbital radius is smaller. This will be relevant to the proposed $\mu^4\text{He}$ and $\mu^3\text{He}$ experiments [7] that aim at measuring the nuclear charge radius of ${}^4\text{He}$ and ${}^3\text{He}$ from the Lamb-shift, to be compared to electron scattering data.

The nuclear electric polarizability of Helium isotopes is interesting for the several above mentioned reasons. It has been already directly measured or extracted from experimental data for the ${}^{3,4,6}\text{He}$ isotopes [1]. In the case of ${}^3\text{He}$ it is worth mentioning that the data from elastic scattering on Pb at energies below the Coulomb barrier [8] are in disagreement with estimates based on

calculations of the photo-absorption cross section [1], the latter being about a factor of 2 smaller. It is also worth noticing that the theoretical calculations are in agreement with photo-absorption experiments, and that the band spanned by using different Hamiltonians in the calculations is smaller than the difference between the data taken from photo-absorption cross section and from ion scattering experiments. The data analysis involved in the latter approach is quite delicate, because one has to separate effects of the nuclear force from Coulomb effects.

In Ref. [9] the polarizabilities of several Hydrogen and Helium isotopes were calculated with *ab-initio* methods. Among the Helium isotopes, ${}^3\text{He}$ and ${}^4\text{He}$ were dealt with, but no prediction for ${}^6\text{He}$ was provided. It is the aim of this paper to fill this gap.

The ${}^6\text{He}$ is known as a halo nucleus, where a tightly bound ${}^4\text{He}$ core is surrounded by two neutrons [10]. It happens to be the lightest of the known halo nuclei and it is a Borromean nucleus, because the two-neutron and neutron-core subsystems are unbound, but the three-body system is held together. Due to the very small separation energy which characterizes halo nuclei, one expects the polarizability of ${}^6\text{He}$ to be much larger than that of the tightly bound ${}^4\text{He}$ isotope. Experimental data indicate this behavior. In this paper we would like to see whether microscopic calculations reproduce the experimental values and lead to a result where $\alpha_E({}^6\text{He}) \gg \alpha({}^4\text{He})$.

We perform a microscopic study of the nuclear polarizability α_E for ${}^6\text{He}$ and compare it to ${}^4\text{He}$. We limit our study to simple semi-realistic two-body forces. For that we use the hyperspherical harmonics method with an effective interaction, EIHH, to speed up the convergence [11, 12]. The polarizability is calculated as a sum rule of the dipole response function using the Lanczos algorithm and also integrating the photo-absorption cross section calculated with the Lorentz integral transform method [13].

This paper is organized as follows. In Section II we describe in details the theoretical calculation of the po-

* E-mail: rgoerke@physics.utoronto.ca

† E-mail: bacca@triumf.ca

‡ E-mail: nir@phys.huji.ac.il

larizability. In Section III we present our results and in Section IV we make a comparison with experiment. Finally, we conclude in Section V.

II. THEORETICAL ASPECTS

The nuclear electric polarizability in the unretarded dipole approximation is defined by the expression

$$\alpha_E = 2\alpha \sum_{n \neq 0} \frac{|\langle n | D_z | 0 \rangle|^2}{E_n - E_0} \quad (1)$$

where α is the fine structure constant, D_z is the unretarded dipole operator and $E_{0/n}$ are the energies of the nuclear ground and excited states $|0\rangle$ and $|n\rangle$, respectively. This observable is clearly related to the photo-absorption cross section and to the dipole response function. The photo-absorption cross section $\sigma_\gamma(\omega)$ of a nucleus is given by

$$\sigma_\gamma(\omega) = 4\pi^2 \alpha \omega R(\omega), \quad (2)$$

where $R(\omega)$ is the response function. In the unretarded dipole approximation

$$R(\omega) = \sum_{n, \bar{0}} |\langle n | D_z | 0 \rangle|^2 \delta(\omega - E_n + E_0), \quad (3)$$

where $\bar{0}$ indicates an average on the initial angular momentum projections. The dipole operator is given by $D_z = \sum_{i=1}^A z_i \tau_i^3 / 2$, where A is the number of nucleons and τ_i^3 and z_i are the third component of the isospin operator and the coordinate of the i th particle in the center of mass frame, respectively. One can recover the expression for α_E in Eq. (1) by calculating sum rules of the photo-nuclear cross section. The various moments of σ_γ are defined as

$$m_n(\bar{\omega}) \equiv \int_{\omega_{th}}^{\bar{\omega}} d\omega \omega^n \sigma_\gamma(\omega), \quad (4)$$

where ω is the photon energy and ω_{th} and $\bar{\omega}$ indicate threshold energy and upper integration limit, respectively. Assuming that $\sigma_\gamma(\omega)$ converges to zero and utilizing the closure of the eigenstates of the nuclear Hamiltonian H , one can relate the polarizability to the $n = -2$ sum rule,

$$\alpha_E = \frac{m_{-2}(\infty)}{2\pi^2} = 2\alpha \sum_n \frac{|\langle n | D_z | 0 \rangle|^2}{E_n - E_0}. \quad (5)$$

The polarizability α_E can be calculated with the Lanczos algorithm using a proper pivot. It is useful to rewrite Eq. (5) as

$$\begin{aligned} \alpha_E &= 2\alpha \langle 0 | D_z^\dagger \frac{1}{H - E_0} D_z | 0 \rangle \\ &= -2\alpha \langle 0 | D_z^\dagger D_z | 0 \rangle \langle \phi_0 | \frac{1}{E_0 - H} | \phi_0 \rangle, \end{aligned} \quad (6)$$

with

$$|\phi_0\rangle = \frac{D_z | 0 \rangle}{\sqrt{\langle 0 | D_z D_z | 0 \rangle}}. \quad (7)$$

Starting from the ‘‘pivot’’ of Eq. (7) where the ground state $|0\rangle$ is obtained by solving the Schrödinger equation, α_E can be expressed as a continued fraction containing the Lanczos coefficients [14]

$$a_i = \langle \phi_i | H | \phi_i \rangle, \quad b_i = \langle \phi_{i+1} | H | \phi_i \rangle, \quad (8)$$

where the $|\phi_i\rangle$ form the Lanczos orthonormal basis $\{|\phi_i\rangle, i = 0, \dots\}$. In fact one has

$$\alpha_E = -2\alpha \langle 0 | D_z^\dagger D_z | 0 \rangle \frac{1}{E_0 - a_0 - \frac{b_1^2}{E_0 - a_1 - \frac{b_2^2}{E_0 - a_3 \dots}}}. \quad (9)$$

In this work we calculate the polarizability in two different ways. On the one hand we utilize Eq. (9). On the other hand we obtain m_{-2} by integrating our results for the total photo-absorption cross section calculated with the Lorentz integral transform (LIT) method [13]. In Ref. [15, 16] we have presented microscopic calculations of the ${}^6\text{He}$ σ_γ with semi-realistic potential models. Here we use larger model spaces which are nowadays available. The LIT, an integral transform with a Lorentzian kernel, is defined as

$$\mathcal{L}(\sigma_R, \sigma_I) = \int d\omega \frac{R(\omega)}{(\omega - \sigma_R)^2 + \sigma_I^2}. \quad (10)$$

The LIT is also typically calculated using the Lanczos technique explained above, (see [17]). In fact it can be re-expressed as

$$\mathcal{L}(\sigma_R, \sigma_I) = -\frac{1}{\sigma_I} \langle 0 | D_z D_z | 0 \rangle \text{Im} \left\{ \langle \phi_0 | \frac{1}{z - H} | \phi_0 \rangle \right\} \quad (11)$$

with $z = E_0 + \sigma_R + i\sigma_I$. It is evident that the LIT in (11) is also a continued fraction as in Eq. (9), where E_0 is replaced by a complex $z = E_0 + \sigma_R + i\sigma_I$. Once $\mathcal{L}(\sigma_R, \sigma_I)$ is calculated, one can invert the LIT [18] to get $R(\omega)$, and thus m_{-2} . The two methods have to agree within the numerical uncertainty. However, with the first method one avoids the complications introduced by the inversion procedure.

Given the Hamiltonian H , the calculation of α_E in both ways is based on the EIH expansion of the wave function. This approach is translational invariant, being constructed with the Jacobi coordinates. We use different semi-realistic potential models for our calculations. Following Ref. [15], we will use the Minnesota (MN) potential [19]

$$\begin{aligned} V_{ij} &= \left[V_R + \frac{1}{2} (1 + P_{ij}^\sigma) V_T + \frac{1}{2} (1 - P_{ij}^\sigma) V_S \right] \times \\ &\quad \left[\frac{1}{2} u + \frac{1}{2} (2 - u) P_{ij}^r \right], \end{aligned} \quad (12)$$

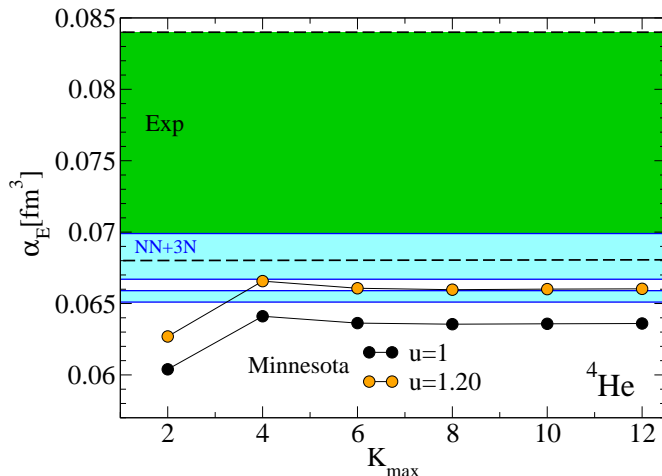


FIG. 1. (Color online) ${}^4\text{He}$ polarizability: calculations with the Minnesota potential for two different u values are shown as a function of the grand-angular momentum quantum number K_{max} . The polarizabilities obtained from realistic two- and three-body interactions [9, 24] are presented as a light (blue) band. Experimental data from [1, 25] are given by the dark (green) band.

where $P_{ij}^{\sigma,r}$ are spin and space-exchange operators, $V_{R,T,S}$ are parameterized as linear combination of Gaussians of the two-body relative distance and u is a parameter. This force reproduces the S -wave nucleon-nucleon phase shifts and correctly binds the deuteron. It renormalizes effects of the tensor force into its central component. A typical value for u in the Minnesota potential is $u = 1$, as we used in [15]. Here we will explore the variation of this parameter by choosing $u \geq 1$. The mixing parameter u does not affect the dominant 1S_0 and 3S_1 waves in the NN interaction, but only affects the $s = 1$, $t = 1$ channels, where the dominant components are the P -waves (1P_1 and ${}^3P_{0,1,2}$). For $u = 1$ there are no P -waves, they contribute only for $u > 1$. Thus, changing u mostly affects ${}^6\text{He}$, without substantially changing ${}^4\text{He}$. Because in [15, 16] we also used the Malfliet-Tjon (MTI-III) [20], and the Argonne AV4' [21] potentials, we will present some results with these interactions as well. The Minnesota potential has been recently used in a microscopic cluster model calculation of ${}^6\text{He}$ [22] and in the Gamow shell model approach [23] for ${}^6\text{He}$ and ${}^8\text{He}$.

III. RESULTS AND DISCUSSION

The main focus of this work is to study the ${}^6\text{He}$ polarizability. We start, however, the discussion with the ${}^4\text{He}$ nucleus. In Fig. 1, we show the results of α_E calculated via the Lanczos coefficients, as in Eq. (9). The ground state $|0\rangle$ and the Lanczos “pivot” $|\phi_0\rangle$ are given in terms of the EIH expansion. While for the ground state the expansion is characterized by an even hyperspherical grand-angular quantum number K_{max} and to-

tal isospin $T = 0$, $T_z = 0$, $D_z|0\rangle$ has to be expanded on odd grand-angular quantum number K'_{max} , where the isospin in the final state is $T' = 1$. Fig. 1 shows the convergence of α_E as a function of K_{max} , where for each point $K_{\text{max}} + 1$ is used for the Lanczos “pivot”. We show our results for the Minnesota potential with $u = 1$ and 1.20 . The convergence is very good, the dependence on u is mild and the results are very close to calculations where realistic nucleon-nucleon (NN) and three-nucleon (3N) forces have been used. For the latter one, results for effective field theory potentials were presented in [9] leading to $\alpha_E = 0.0683(8)(14) \text{ fm}^3$ (corresponding to the upper light (blue) band in Fig. 1). The error bar of this calculation is accounting for the convergence error 0.0008 fm^3 and also for the uncertainty in the underlying dynamics 0.0014 fm^3 . We also show the results of α_E for the Argonne v_{18} two-body force and Urbana IX three-body force of Ref. [24] leading to $\alpha_E = 0.0655(4)$ (corresponding to the lower light (blue) band in Fig. 1), where the error bar comes from convergence only. The experimental data are shown as a darker (green) band. These include the more recent evaluation of Ref. [1] based on the Arkatov *et al.* [26] experimental measurement of the photo-absorption cross section and an older result reported in Ref. [25], based on earlier measurements by Arkatov *et al.* [27]. We would like to point out that the semi-realistic Minnesota potentials lead to a value of the polarizability which is consistent with realistic calculations and is only about 15% smaller than the average value in the experimental band.

We can also calculate the polarizability by integrating the photoabsorption cross section obtained with the LIT method. We get perfect agreement as with the Lanczos coefficients. For example, for the standard Minnesota potential where $u = 1$ and for a $K_{\text{max}} = 12/13$ model space, the Lanczos method gives $\alpha_E = 0.06360 \text{ fm}^3$ and integrating σ_γ up to 120 MeV we get 0.06336 fm^3 , with just a 0.4% difference.

Now we move to the ${}^6\text{He}$ nucleus. We first calculate α_E from the Lanczos coefficients. Also in this case the ground state is expanded on even hyperspherical grand-angular quantum number K_{max} , but the total isospin is $T = 1$, $T_z = -1$, and $D_z|0\rangle$ is expanded on odd $K'_{\text{max}} = K_{\text{max}} + 1$. In this case though, the final isospin can be $T' = 1$ or $T' = 2$. This leads to two possible isospin channels that are calculated separately and that open up at different energies. Experimentally, the $T = 1$ channel opens up at photon energy $\omega_{th} = 0.975 \text{ MeV}$, while the $T = 2$ channel opens up at $\omega_{th} = 22.77 \text{ MeV}$, with $\gamma {}^6\text{He} \rightarrow {}^3\text{H} n n p$. Due to the inverse energy weight in Eq. (5), the $T = 2$ channel is expected to be less relevant to α_E . From our calculations we find that the percentage contribution of the $T=2$ isospin channel to the total polarizability changes from 2% to 4% when varying u from 1 to 1.20 in the Minnesota potential.

In Fig. 2, we present a similar plot as in Fig. 1 for ${}^6\text{He}$ with semi-realistic interactions. We observe a much slower convergence of α_E for ${}^6\text{He}$ than for ${}^4\text{He}$ with all

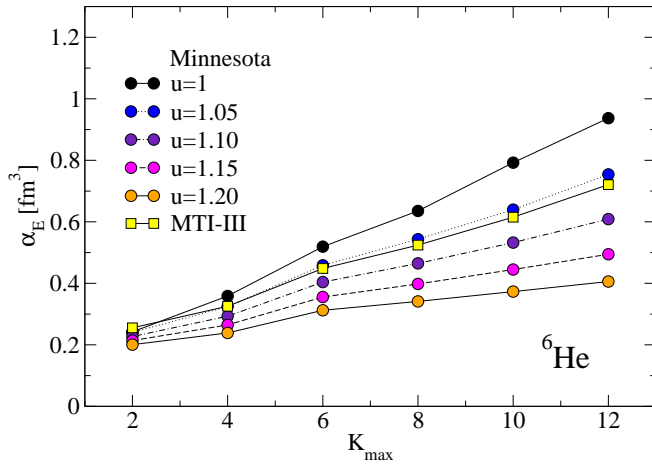


FIG. 2. (Color online) The polarizability of ${}^6\text{He}$ as a function of the grand-angular momentum K_{max} for different semi-realistic interactions: the Minnesota potential with $u = 1 - 1.2$ and the MTI-III potential.

TABLE I. Results of the EIHH calculation with $K_{\text{max}} = 12$ for the different u value of the Minnesota potential. The values for the energies are in MeV.

Potential	$E_0({}^4\text{He})$	$E_0({}^6\text{He})$	$S_{2n}({}^6\text{He})$
Minnesota			
$u=1.00$	-29.949	-30.45	0.50
$u=1.05$	-29.978	-31.13	1.15
$u=1.10$	-30.007	-31.88	1.87
$u=1.15$	-30.037	-32.72	2.68
$u=1.20$	-30.069	-33.65	3.59
MTI-III	-30.760	-32.24	1.48

the potentials employed. By looking at the different u values in the Minnesota potential, we see that the convergence rate and the value of α_E substantially change with u . This is related to the variation of the binding energy, and consequently of the two-neutron separation energy, whose numerical values are shown in Table I for completeness. By increasing u we are adding more P -wave interactions, which bring additional binding to the ${}^6\text{He}$ nucleus, while leaving ${}^4\text{He}$ almost unaffected. Naively, this makes ${}^6\text{He}$ more tightly bound and thus more difficult to polarize, i.e., α_E gets smaller. For the value of $u = 1$ the convergence of the polarizability is particularly slow, due to the fact that ${}^6\text{He}$ is barely bound, with $S_{2n} = 0.56$ MeV which is about a factor of 2 smaller than the experimental value. With the MTI-III potential we get a convergence pattern which is close to the Minnesota potential for $u = 1.05$, because the prediction of S_{2n} is similar with these two potentials, see Table I. The information that one gains from Fig. 2 is that by increasing S_{2n} we can change the overall slope of the convergence pattern of α_E .

For any considered value of u though, it is clear that

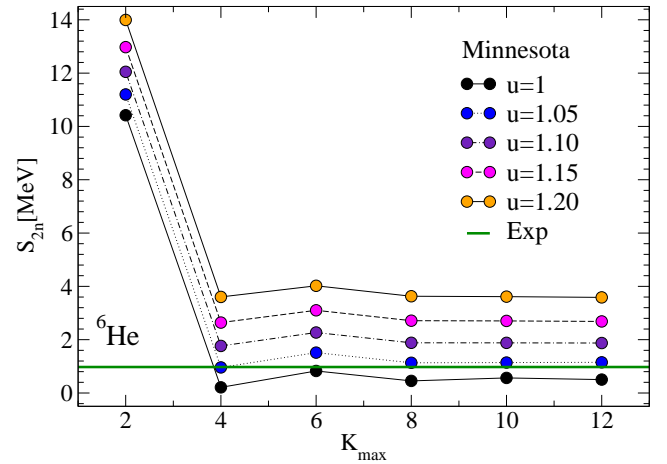


FIG. 3. (Color online) ${}^6\text{He}$ two-neutron separation energy as a function of the grand-angular momentum K_{max} for the Minnesota potential and different u parameters. The experimental value is also shown.

our calculations reproduce the fact that the polarizability of the halo nucleus of ${}^6\text{He}$ is much larger than that of the tightly bound ${}^4\text{He}$, the ratio being almost an order of magnitude.

Here we would like to point out that Brida and Nunes in [22] have used the Minnesota potential with $u = 1.15$ in a microscopic cluster model and obtained a separation energy $S_{2n} = 0.90(5)$ MeV. This result is different from the value we obtain and report in Table I. Their calculation is performed without the Coulomb force, but its effect cancels in the separation energy. Because for ${}^4\text{He}$ the value reported in [22] for the binding energy is -30.85 MeV, which is in agreement with our value of -30.86(1) (with no Coulomb force), we think that the difference is due to the cluster assumption made for ${}^6\text{He}$. We do not make such assumption and in convergence, the EIHH result is exact. In Fig. 3, we show that the separation energy S_{2n} is very well converged within the model space available for all these potentials.

We can also calculate the polarizability by integrating the photoabsorption cross section obtained with the LIT method and compare it to the above results. We quote numbers for the Minnesota potential with $u = 1.05$ in the largest available model space $K_{\text{max}} = 12/13$. The Lanczos method gives $\alpha_E = 0.7542$ fm³ and integrating σ_γ up to 40 MeV (60 MeV) we get 0.7711 fm³ (0.7827) fm³. Integrating the cross section we have a 3-4% difference, which is due to the fact that LIT is not completely converged and the inversion procedure introduces some numerical error.

Now we would like to investigate the dependence of the polarizability on the two-neutron separation energy. This can be achieved for example by plotting α_E versus S_{2n} for the different values of the parameter u in the Minnesota potential. In Fig. 4, we can see that we find a correlation between α_E and S_{2n} . Calculations have been performed with $K_{\text{max}} = 12$ ($K'_{\text{max}} = 13$). As an esti-

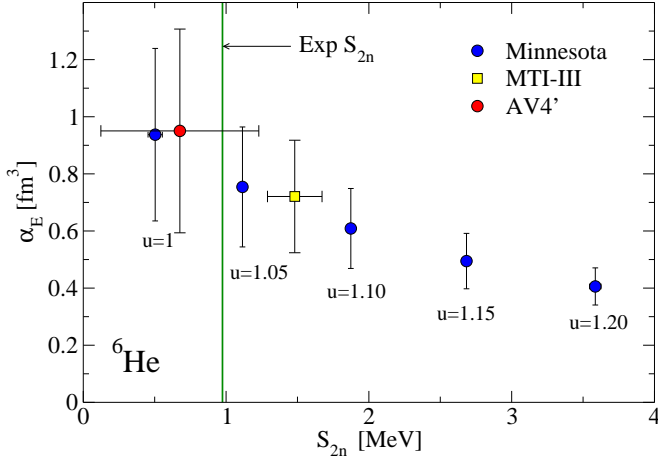


FIG. 4. (Color online) Correlation between α_E and S_{2n} in ${}^6\text{He}$ obtained with the Minnesota potential varying the parameter u . The MTI-III and AV4' results are also shown.

mate of the theoretical error bar in the few-body method we take the difference between the largest possible calculation with $K_{\text{max}} = 12$ and the $K_{\text{max}} = 8$ result. We also present the data for the MTI-III and AV4' potential (as used in [16]) for completeness. The error bars for the polarizability increase as the separation energy gets smaller. This is a reflection of the slower convergence observed in Fig. 2. For the Minnesota potential S_{2n} has a negligible error, hardly visible in Fig. 4. For the MTI-III and AV4' potentials the error in S_{2n} is large because these interaction models are not as soft as the Minnesota force.

In Ref. [9] it was argued that the polarizability should roughly scale like the inverse square of the binding energy of a nucleus. For a halo system, like ${}^6\text{He}$, the relevant scale parameter is the separation energy, rather than the binding energy. The $\alpha_E - S_{2n}$ dependence empirically observed in Fig. 4 is compatible with such a behavior.

In order to reproduce the polarizability of a halo nucleus, it is expected that the halo structure, thus S_{2n} , should be correctly modeled, even if the absolute binding of ${}^4\text{He}$ and ${}^6\text{He}$ are not reproduced. Thus, one can estimate the value of α_E by choosing S_{2n} to be around the experimental value and then calculate the corresponding polarizability. A value of u that gives S_{2n} close to experiment is $u = 1.05$, where the convergence of α_E is slower than for larger values of u . From a closer look to Fig. 2 and Fig. 3 we can see that also for $u = 1.20$ the polarizability α_E is still increasing when K_{max} becomes larger, even though the separation energy is converged. This means that the convergence of the polarizability is not only influenced by S_{2n} . Other observable that is naturally related to the polarizability in the unretarded dipole approximation is the radius operator.

In recent papers [28, 29] the correlation between the polarizability and the neutron skin of the ${}^{208}\text{Pb}$ nucleus was studied within the nuclear density functional theory framework. In the following, we will investigate the same

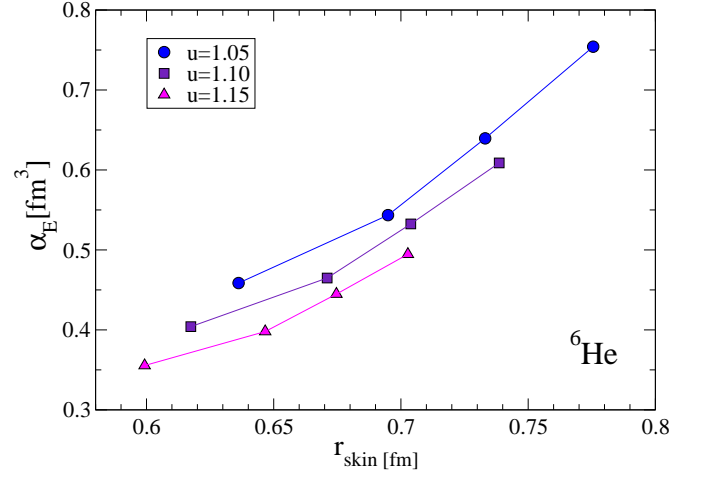


FIG. 5. (Color online) Correlation between the nuclear electric polarizability of ${}^6\text{He}$ and the skin radius with the Minnesota potential with different u . The four points for each u value correspond to calculations with $K_{\text{max}} = 6, 8, 10$ and 12 , moving from the left to the right.

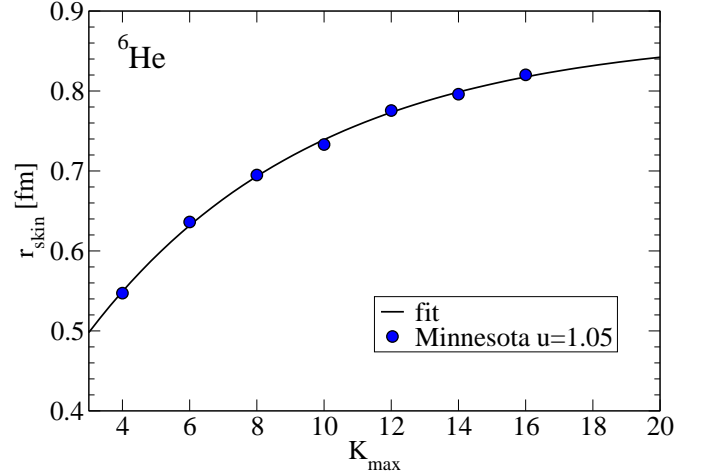


FIG. 6. (Color online) Neutron skin radius r_{skin} of ${}^6\text{He}$ with the Minnesota potential and $u = 1.05$, as a function of the grand-angular momentum quantum number K_{max} . The curve is a fit to the calculated points, used to extrapolate to infinite model space.

correlation for ${}^6\text{He}$, even though ${}^6\text{He}$ is a different system. For halo nuclei, one refers to the halo radius, rather than the skin radius, but clearly the observable

$$r_{\text{skin}} = r_n - r_p, \quad (13)$$

where r_n and r_p are the mean point-neutron and point-proton radii, can be uniquely defined. In our recent work [30], such observables have been calculated for ${}^6\text{He}$ from realistic two-body potentials in the EIH method. Here, instead, we use the same semi-realistic interaction as for the α_E calculations. In Fig. 5, we show a plot of α_E versus r_{skin} for different model spaces and for three different values of u in the Minnesota potential. The four

points for each u value correspond to calculations with $K_{\max} = 6, 8, 10$ and 12 , from the lowest to the largest value of α_E , respectively. For $K_{\max} \geq 8$ we clearly see a linear dependence between α_E and r_{skin} for all the three u values where the coefficients depend on the separation energy as

$$\alpha_E = a(S_{2n}) + b(S_{2n})r_{\text{skin}}. \quad (14)$$

Because S_{2n} is converged and because of the linear dependence displayed in Fig. 5 we deduce that the calculation of α_E is not fully converged because the radii, and especially r_n , are not fully converged. The calculation of a radius of the ground state does not require an expansion on the dipole excited states as in Eq. (7) and as such is less computation demanding and can be performed for larger model spaces, where radii are better converged. Thus, the approach we take to estimate α_E from our calculations is to fit the coefficients $a(S_{2n})$ and $b(S_{2n})$ from the α_E results in the available model spaces and, assuming that this physical linear dependence will be unchanged in larger model spaces, we will use the coefficients to obtain α_E from a bound state calculation of r_{skin} . Starting with $u = 1.05$, so that S_{2n} is close to experiment, we fit the parameters a and b to the results of our calculations using the available values of $K_{\max} \geq 6$. We test this procedure on the available model space by varying the largest K_{\max} . For a model space with largest $K_{\max} = 10$, we obtain $a = -0.7 \pm 0.2 \text{ fm}^3$ and $b = 1.83 \pm 0.3 \text{ fm}^2$ fitting to three points, $K_{\max} = 6, 8, 10$. Using these values and the value $r_{\text{skin}} = 0.776 \text{ fm}$, calculated in the next largest model space $K_{\max} = 12$, our linear ansatz of Eq. (14) yields $\alpha_E = 0.7 \pm 0.3 \text{ fm}^3$. The calculated value of α_E from the hyperspherical harmonics expansion up to $K_{\max} = 12$ is 0.754 fm^3 , which is within our estimated error band. Now we will repeat this procedure utilizing our best three values $K_{\max} = 8, 10, 12$ (we omitted the $K_{\max} = 6$ point as it does not fall in line with the other points). The resulting values are $a = -1.27 \pm 0.04 \text{ fm}^3$ and $b = 2.62 \pm 0.05 \text{ fm}^2$. We then calculate r_{skin} up to the largest grand-angular momentum value accessible with our computational facility, $K_{\max} = 16$. Using the corresponding $r_{\text{skin}} = 0.82 \text{ fm}$ and propagating the fit errors on a and b in the linear ansatz, we obtain $\alpha_E = 0.88 \pm 0.06 \text{ fm}^3$. Concerning the skin radius, one can clearly see from Fig. 6, that convergence is approached. Extrapolating these points with an exponential *ansatz* of the form $r_{\text{skin}}(K_{\max}) = r_{\text{skin}}(\infty) - ce^{-\kappa K_{\max}}$ we get $r_{\text{skin}}(\infty) = 0.87(5) \text{ fm}$. As an error estimate we take the difference between $r_{\text{skin}}(K_{\max} = 16)$ and $r_{\text{skin}}(K_{\max} = 12)$. The theoretical value is somehow larger than the experimental data. In fact, combining different measurements of the matter radius [31–33] with the most recent evaluation of the proton radius [5], one can infer r_n and consequently the skin radius, which is found to be $0.52 \leq r_{\text{skin}}^{\text{exp}} \leq 0.62 \text{ fm}$. The variation on $r_{\text{skin}}^{\text{exp}}$ is fairly large, due to the large uncertainty in the matter radius determination from ion scattering.

Because the extrapolated skin radius is our best es-

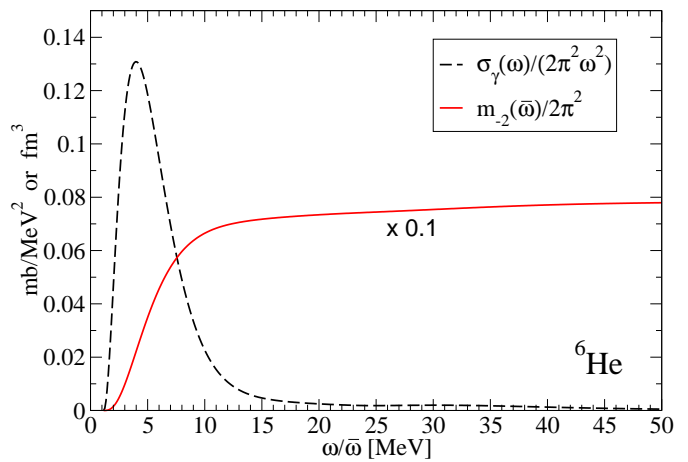


FIG. 7. (Color online) Double inverse energy weighted cross section as a function of the energy ω and sum rule $m_{-2}(\bar{\omega})/2\pi^2$ as a function of $\bar{\omega}$ for ${}^6\text{He}$ with the Minnesota potential and $u = 1.05$.

timate of this observable, we use this value in Eq. (14) and propagate its error estimating the polarizability, considering it independent from the fit errors on a and b . Finally, our estimate of the theoretical nuclear electric polarizability of ${}^6\text{He}$ is $\alpha_E = 1.00(14) \text{ fm}^3$. This value is consistent with what we obtained without extrapolating the radius, showing that the error bars are based on conservative estimates. If we were to use Eq. (14) with the experimental values of the skin radius, one would obtain a nuclear electric polarizability of $\alpha_E = 0.08 - 0.34 \text{ fm}^3$, which is even smaller than the estimate based solely on theory.

IV. COMPARISON WITH EXPERIMENT

In Ref. [1] an evaluation of the experimental number for the polarizability of ${}^6\text{He}$ was presented, leading to $\alpha_E^{\text{exp}} = 1.99(40) \text{ fm}^3$. This was obtained from the inverse energy weighted integral of experimental and theoretical $B(E1)$ response functions for ${}^6\text{He}$. The experimental distribution was measured by Aumann *et al.* [34] from the Coulomb breakup of ${}^6\text{He}$ on Lead and Carbon at $240 \text{ MeV}/u$ up to 8 MeV above threshold. In order to obtain the polarizability, data were extrapolated up to 12.3 MeV , where the threshold for the breakup into two tritons opens up. The theoretical curve was taken from a calculation of the dipole transition to the 1^- continuum [35] in a three-body model with phenomenological $n-n$ and $n-\alpha$ interactions plus an effective three-body force, also calculated up to the two tritons threshold. The estimate was done in two steps: (i) an average of the experimental data and theoretical curve was taken up to 12.3 MeV ; (ii) to account for the higher energies, the polarizability of ${}^4\text{He}$ was added. The latter one basi-

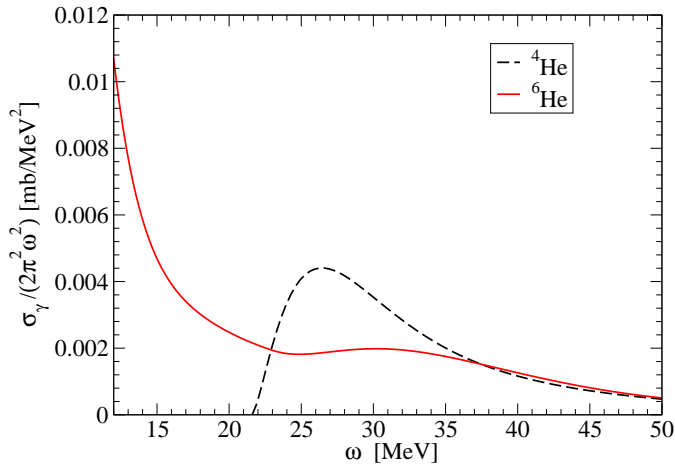


FIG. 8. (Color online) Double inverse energy weighted cross section as a function of the energy ω for ^4He and ^6He with the Minnesota potential and $u = 1.05$.

cally comes from integrating the photo-dissociation data from Arkatov *et al.* [26]. Because we can access the full response functions using the LIT method at any energy below the pion production threshold, we can verify these two approximations. First, it is interesting to study the convergence of α_E calculated as a sum rule of the response, see Eq. (4) and (5), to investigate the validity of (i). In Fig. 7, we present both the integrand function $\sigma_\gamma(\omega)/2\pi^2\omega^2$ versus ω and the convergence of the integral $m_{-2}(\bar{\omega})/2\pi^2$ versus $\bar{\omega}$. At $\bar{\omega} = 8$ MeV the sum rule is exhausted only up to 75%. Thus only 75% of the α_E^{exp} is based solely on experimental data. At $\bar{\omega} = 12.3$ MeV, where the two ^3H channel opens up the sum rule is exhausted up to 90%. We observe that one needs to integrate up to 40 MeV of energy to have the sum rule exhausted at the 98% level.

To verify the approximation (ii) we can compare the integrand function $\sigma_\gamma(\omega)/2\pi^2\omega^2$ for ^6He and ^4He at energies beyond 12.3 MeV. In Fig. (8) we observe that the two curves agree with each other for $\omega > 35$ MeV, where the sum rule is almost exhausted. In the region beyond the ^4He disintegration threshold and below about 35 MeV one would over estimate the sum rule integrating the ^4He curve, because one gets 0.044 fm^3 , to be compared to the 0.027 fm^3 obtained when correctly integrating the ^6He curve. On the other hand, neglecting the part of the cross section for $\omega > 12.3$ MeV and below the ^4He disintegration threshold one underestimates the sum rule. The contribution of this portion is 0.037 fm^3 , about 5% of the sum rule. These two effects almost cancel out so that, the approximation (ii) does not lead to a big error.

We think that the main reason of the disagreement

between the estimate from Ref. [1] and our calculations comes from the difference in the low-energy part of the response. In our previous work [15, 16] we have shown that our calculations with semi-realistic potentials underestimates the data from Aumann *et al.* [34]. Thus, what we observe for the polarizability is consistent with this fact. We would like to point out that (i) nuclear corrections might affect the results in the ion scattering experiment of [34] and that (ii) as discussed earlier, similar experiments for ^3He lead to large discrepancy with photo-dissociation results. Nevertheless, measuring α_E from the dipole response function it would be desirable to have data up to higher energies than 12.3 MeV. Additional or alternative measurements of α_E would help to better constrain this observable.

V. CONCLUSIONS

We summarize our results as follows. We have carried out an estimate of the nuclear polarizability of ^6He based on the hyperspherical harmonics expansion with simple semi-realistic potentials. Our calculations clearly reproduce the fact that the polarizability of the halo nucleus of ^6He is much larger than that of the tightly bound ^4He . For ^4He the semi-realistic Minnesota potentials lead to a value of the polarizability which is consistent with realistic calculations and is about 15% smaller than the average value in the experimental band. Nevertheless, a large disagreement is found for ^6He . In order to estimate α_E we have chosen a potential that reproduces the separation energy and then we investigated the correlation of the polarizability with the skin radius. Our final result is $\alpha_E = 1.00(14) \text{ fm}^3$, which is about a factor of 2 smaller than the estimates from experimental data. This points towards a disagreement of microscopic theory and experiments. To shed light on this, it would be nice to have more data or alternative measurements of α_E . Concerning the theoretical calculations, it is desirable to extend these results to realistic potentials including also three-body forces. We leave this subject to a future work.

VI. ACKNOWLEDGMENT

The work of R. Goerke and S. Bacca was supported in part by the Natural Sciences and Engineering Research Council (NSERC) and in part by the National Research Council of Canada. The work of N. Barnea was supported by the ISRAEL SCIENCE FOUNDATION (grant no. 954/09). Numerical calculations were performed at TRIUMF.

[1] K. Pachucki, A.M. Moro, Phys. Rev. A **75**, 032521 (2007).

[2] A. Tamii *et al.*, Phys. Rev. Lett. **17**, 062502 (2011).

- [3] W. Nöckerhäuser *et al.*, Phys. Rev. A **83**, 012516 (2011).
- [4] L. B. Wang *et al.*, Phys. Rev. Lett. **93**, 142501 (2004).
- [5] M. Brodeur *et al.*, Phys. Rev. Lett. **108**, 052504 (2012).
- [6] P. Mueller *et al.*, Phys. Rev. Lett. **99**, 252501 (2007).
- [7] A. Antognini *et al.*, Can. J. Phys. **89**, 47 (2011).
- [8] F. Goeckner, L. O. Lamm, and L. D. Knutson, Phys. Rev. C **43**, 66 (1991).
- [9] I. Stetcu, S. Quaglioni, J.L. Friar, A.C. Hayes, and P. Navratil, Phys. Rev. C **79**, 064001 (2009).
- [10] I. Tanihata, J. Phys. G **22**, 157 (1996).
- [11] N. Barnea and A. Novoselsky, Phys. Rev. A **57**, 48 (1998); Ann. Phys. (N.Y.) **256**, 192 (1997).
- [12] N. Barnea, W. Leidemann, and G. Orlandini, Phys. Rev. C **61**, 054001 (2000); Nucl. Phys. **A693**, 565 (2001).
- [13] V.D. Efros, W. Leidemann, and G. Orlandini, Phys. Lett. **B338**, 130 (1994).
- [14] E. Dagotto, Rev. Mod. Phys. **66**, 763 (1994), and references therein.
- [15] S. Bacca, M. A. Marchisio, N. Barnea, W. Leidemann and G. Orlandini, Phys. Rev. Lett. **89**, 052502 (2002).
- [16] S. Bacca, N. Barnea, W. Leidemann and G. Orlandini, Phys. Rev. C **69**, 057001 (2004).
- [17] M. A. Marchisio, N. Barnea, W. Leidemann, and G. Orlandini, Few-Body Syst. **33**, 259 (2003).
- [18] V.D. Efros, W. Leidemann, and G. Orlandini, Few-Body Syst. **26**, 251 (1999); D. Andreasi, W. Leidemann, C. Reiss, and M. Schwamb, Eur. Phys. J. **A24**, 361 (2005).
- [19] D.R. Thompson, M. LeMere and Y.C. Tang, Nucl. Phys. **A286**, 53 (1977).
- [20] R. A. Malfliet and J. A. Tjon, Nucl. Phys. **A127**, 161 (1969).
- [21] S.C. Pieper, and R.B. Wiringa, Phys. Rev. Lett. **89** (2002) 182501.
- [22] I. Brida and F.M. Nunes, Nucl. Phys. A **847**, 1 (2010).
- [23] G. Papadimitriou, A. T. Kruppa, N. Michel, W. Nazarewicz, M. Płoszajczak and J. Rotureau, Phys. Rev. C **84**, 051304 (2011).
- [24] D. Gazit, N. Barnea, S. Bacca, W. Leidemann, and G. Orlandini, Phys. Rev. C **74**, 061001 (2006).
- [25] J. L. Friar, Phys. Rev. C **16**, 1540 (1977).
- [26] Yu.M. Arkatov, P.I. Vatsset, V.I. Voloshchuk, V.A. Zolenko, and I.M. Prokhorets, Yad. Fiz. **31**, 1400 (1980) [Sov. J. Nucl. Phys. **31**, 726 (1980)].
- [27] Yu.M. Arkatov, *et al.*, Yad. Fiz. **19**, 1172 (1974) [Sov. J. Nucl. Phys. **19**, 598 (1974)].
- [28] J. Piekarewicz, B. K. Agrawal, G. Coló, W. Nazarewicz, N. Paar, P.-G. Reinhard, X. Roca-Maza, and D. Vretenar, Phys. Rev. C **85**, 041302 (2012).
- [29] S. Shlomo and M. R. Anders, private communication.
- [30] S. Bacca, N. Barnea, A. Schwenk, arXiv:1202.0516.
- [31] I. Tanihata, D. Hirata, T. Kobayashi, S. Shimomura, K. Sugimoto and H. Toki, Phys. Lett. B **289**, 261 (1992).
- [32] G. D. Alkhazov, *et al.*, Phys. Rev. Lett. **78**, 2313 (1997).
- [33] O. A. Kislev, *et al.*, Eur. Phys. J. A **25**, 215 (2005).
- [34] T. Aumann *et al.*, Phys. Rev. C **59**, 1252 (1999).
- [35] I.J. Thompson, B.V. Danilin, V.D. Efros, J.S. Vaagen, J.M. Bang, and M.V. Zhukov, Phys. Rev. C **61**, 024318 (2000).